Oceland: A conceptual model for ocean-land-atmosphere interactions based on water balance equations

Luca Schmidt[a] , Cathy Hohenegger[a]

[a] *Max Planck Institute for Meteorology, Hamburg*

Corresponding author: Luca Schmidt, luca.schmidt@mpimet.mpg.de

ABSTRACT: Which ~~processes or physical quantities~~ control the partitioning of precipitation between land and ocean? ~~What~~ large-scale constraints ~~on this partitioning~~ exist? We address these questions using a conceptual box model based on water balance equations. With a small number of empirical but physically motivated parametrizations of the water balance components, we construct a set of coupled ordinary differential equations which describe the dynamical behavior of the water vapor content of land and ocean atmospheres as well as the land's soil moisture content. For a model configuration with one ocean and one land domain and periodic boundary conditions, we compute equilibrium solutions across the parameter space and analyze the sensitivity of the equilibrium state to parameter choices. The precipitation partitioning is quantified by the precipitation ratio, PR ~~$\equiv P_\ell/P_o$, where P_ℓ and P_o denote~~ spatially averaged land and ocean precipitation rates in equilibrium, ~~respectively.~~ We find that PR is primarily controlled by an atmospheric transport parameter, followed by the land fraction, and to an even lesser extent by various soil parameters. The precipitation ratio is confined to a range between zero and one ~~which is consistent with observational estimates for the tropics. We are able to explain this range based on the underlying equations and model assumptions.~~ Since precipitation ratios larger than one have been observed for local systems such as tropical islands, ~~we explore pathways through which land precipitation can become stronger than ocean precipitation in the proposed water balance model. One way is to relax certain model assumptions, for instance by using different parametrizations for land and ocean precipitation or by introducing a diurnal cycle and accounting for the effect of sea-breezes. Another way is to model local systems as open systems which are embedded in a large-scale environment that provides atmospheric boundary conditions. We demonstrate that an open model configuration with an island between two ocean boxes~~ is able to produce precipitation ratios larger than one but ~~that~~ such solutions arise from only a small subset of model parameter choices characterised by rather small land fractions and sufficiently large ~~water vapor pass values at the windward model boundary.~~

1. Introduction

All water that evaporates from Earth's land and ocean surfaces must eventually return to the surface as precipitation but which physical processes or individual quantities determine how precipitation gets partitioned between land and ocean? Existing literature provides little information to answer this seemingly simple question. We address this lack of understanding by representing the coupled land-ocean-atmosphere system by a simple conceptual box model which is governed by water balance equations as e.g. described in Peixóto and Oort (1983). Expressing the water balance components by empirical but physically motivated parametrizations and analyzing equilibrium solutions across the entire sensible parameter space, we are able to put constraints on the ratio between mean land and ocean precipitation, PR, which are reasonably close to observed values.

Such observational values have rarely been reported in previous studies but FIEDLER ET AL. and HOHENEGGER ET AL. present values for the tropics close to $PR = 1$. These values, reflecting nearly equal mean rain rates over land and ocean, are somewhat surprising given that the two surface types have very different characteristics and interact with the atmosphere in different ways. Most notably, the land can dry out and thereby significantly reduce the moisture input into the atmosphere through evapotranspiration while the ocean is constantly saturated evaporates water at a nearly constant rate. We would expect such differences to leave a mark in the precipitation signal. If mean rain rates are nevertheless almost identical over land and ocean, do we overestimate the influence of surface properties on large spatial and temporal scales? Our conceptual framework allows for the investigation of the sensitivity of the model's equilibrium solution to the choice of parameter values and thereby for the identification of the physical properties that primarily control the precipitation partitioning.

Conceptual models have widely been used in hydrological studies. In a seminal paper, Budyko and Drozdov (1953) introduced a one-dimensional model of land-atmosphere interactions in which an airstream with a given moisture content at the windward boundary traverses a continental region and moistens or dries along the passage depending on the relative magnitude of mean precipitation and surface evapotranspiration in the region. Since precipitation in this framework can be described as the sum of imported moisture from outside the model domain (e.g. from an ocean) and locally evaporated moisture from within the region, this so-called "Budyko model" was used and further developed in several studies that assessed the importance of local moisture

recycling for precipitation in a given land area (see Burde and Zangvil (2001) for a review of different adaptations of the Budyko model and its general limitations).

Such Budyko-type studies come in two kinds: The first kind, including Brubaker et al. (1993), Eltahir and Bras (1994) and Ent et al. (2010), quantifies the water balance components using observations. These studies find that precipitation recycling is important for land precipitation, especially in hotspot regions of land-atmosphere interaction such as the Sahel region, the Amazon and mountainous regions in Asia. The second kind uses empirical parametrizations for the water balance components, enabling a dedicated sensitivity analysis which aids conceptual understanding more directly. Examples are Rodriguez-Iturbe et al. (1991) and Entekhabi et al. (1992) who investigated the soil moisture dynamics of droughts. We adopt this latter approach but extend the soil moisture model of Rodriguez-Iturbe et al. (1991) by additional atmospheric moisture balance equations with suitable parametrizations of advection and precipitation which are functions of the mean atmospheric water content over land and ocean. This is necessary because we are not only interested in the vertical interaction between land surface and atmosphere for which moisture advection at the windward model boundary could be assumed known and constant but also in the horizontal interaction between land and ocean atmospheres that requires a dynamic formulation of advection. To our knowledge, the combination of vertical and horizontal coupling in a land-ocean-atmosphere system has not been studied with a conceptual model before.

2. Model description

To understand the controlling factors for precipitation partitioning between land and ocean and whether fundamental constraints for this partitioning arise from water balance equations, we propose a box model as sketched in Figure 1. The model consists of an ocean domain denoted by subscript 'o', and a land domain denoted by subscript 'l' ~~with a relative size~~ given by the land fraction parameter α. Each of the two domains contains a ground box at the bottom (ocean or land) and an atmospheric box aloft. While the horizontal extent of the full model domain is prescribed by length L, the vertical extent of the ground and atmospheric boxes is taken to be infinite in downward and upward direction, respectively. The model has periodic boundary conditions, i.e. topologically, it resembles the wall of a cylinder with the right boundary of the land domain, B_1 being identical with the left boundary of the ocean domain. This turns the model into a closed

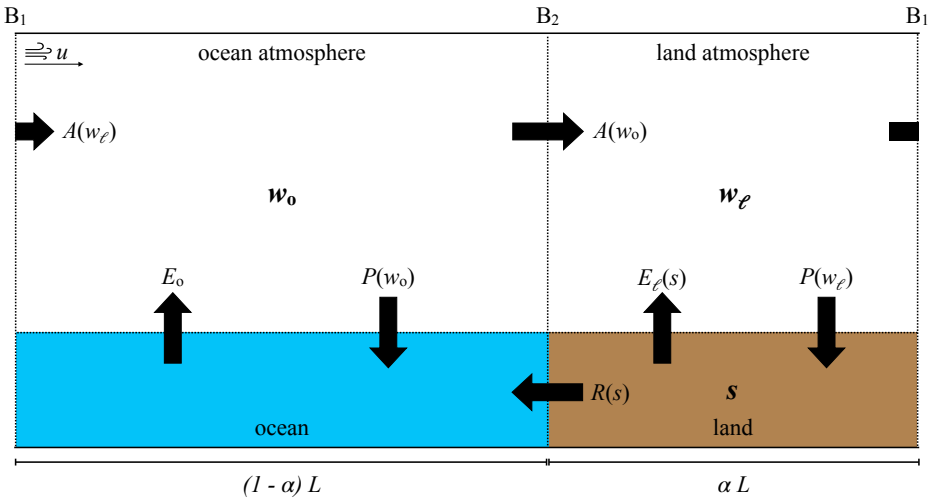

FIG. 1. Model sketch of the land-ocean-atmosphere system with periodic boundary conditions. Black arrows represent the mean water fluxes between the four model boxes. With the exception of ocean evaporation E_o, which is treated as a constant model parameter, all fluxes are functions of the relative soil moisture saturation, s, or integrated water vapor passes of land and ocean atmospheres, w_ℓ and w_o, respectively. The atmospheric moisture transport is driven by a constant mean horizontal background wind speed, u.

system in which water is conserved and which does not interact with any external environment. Such a *closed* model (CM) is suitable to describe, for example, the entire ~~globe~~ or - if net moisture exchange with the Extratropics is negligible - the ~~tropical band~~. Later, in section 6, we discuss a possible formulation for an *open* model (OM) ~~which is a better representation of regional systems. In the case of an open model for small spatial scales, boundary values are provided by synoptic-scale conditions and the modelled region can act as a net source or sink of atmospheric moisture. In this case, water is still conserved in a global sense but not necessarily within the modelled domain.~~

a. Water balance equations

~~We further~~ assume that the model boxes have well-mixed properties and that all water fluxes between them can be expressed as functions of their mean moisture ~~content, i.e. the moisture state of the boxes~~. For atmospheric boxes, we use the mean water vapour pass w in mm, and for the land box the unitless mean relative soil moisture saturation s to describe the moisture state. As the ocean is considered fully saturated at all times, we don't need to assign a moisture variable to

it. Hence, the full information on the moisture state of the land-ocean-atmosphere system at any given time t in days is given by the set of state variables $\{w_o(t), w_\ell(t), s(t)\}$.

Following earlier studies by Peixóto and Oort (1983) and Brubaker et al. (1991), we describe the time-evolution of the state variables by coupled water balance equations in which moisture sinks and sources are represented by water fluxes between the boxes:

$$\frac{ds}{dt} = \frac{1}{nz_r}\left[P(w_\ell) - R(s, w_\ell) - E_\ell(s)\right] \tag{1}$$

$$\frac{dw_\ell}{dt} = E_\ell(s) - P(w_\ell) + A_\ell(w_\ell, w_o) \tag{2}$$

$$\frac{dw_o}{dt} = E_o - P(w_o) + A_o(w_\ell, w_o). \tag{3}$$

Note that the time-dependence of s, w_ℓ and w_o is implicit in Equations (1) to (3). The relevant fluxes, which are indicated by black arrows in Figure 1 ~~and given as spatial mean flux rates in mm/day ('mean' being frequently omitted in the remainder of this text),~~ are precipitation P from atmosphere to ground boxes, evapotranspiration E_ℓ from soil to land atmosphere, ocean evaporation E_o to the ocean atmosphere, runoff R from soil to ocean and advection A between the atmospheric boxes. The advection terms A_ℓ and A_o in Eqns. (2) and (3) refer to the *net* advection ~~rate~~ into the land and ocean atmosphere, respectively, and are positive for a net moisture import and negative for net moisture export. ~~Note that the total advection~~ in a closed system vanishes, i.e. $\alpha A_\ell + (1-\alpha)A_o = 0$. ~~Dimensionless soil porosity n times hydrologically active soil depth z_r in mm is a constant model parameter.~~ An implicit assumption of this water balance approach is that the water holding capacity of the atmosphere does not change significantly over long enough timescales which we consider here.

b. ~~Parametrizations~~

While the conservation of water is a fundamental condition, there are no simple fundamental laws governing the water fluxes between the model boxes. Instead, we need to turn to empirical relationships between the flux quantities and moisture state variables, as has been previously done by Rodriguez-Iturbe et al. (1991). ~~We adopt the parametrization of~~ runoff ~~as~~ the fraction R_f of precipitation that does not infiltrate the soil,

$$R(s, w_\ell) = R_\mathrm{f}(s) P(w_\ell), \tag{4}$$

with

$$R_\mathrm{f}(s) = \epsilon s^r, \tag{5}$$

and the two dimensionless parameters ϵ and r. Equation (5) tells us that runoff intensifies as the soil moistens. Precipitation and runoff in Eqn. (1) ~~can be combined to~~ $P(w_\ell) - R(s, w_\ell) = P(w_\ell)\Phi(s)$, where we introduce the infiltration function $\Phi(s) = 1 - R_\mathrm{f} = 1 - \epsilon s^r$. This parametrization assumes that runoff discharge happens uniformly across the land domain and that its water does not participate in any secondary processes that could moisten the soil.

For precipitation, Rodriguez-Iturbe et al. (1991) followed the approach of Budyko and Drozdov (1953) ~~who obtained an expression for precipitation that solely depends on soil moisture and fixed model parameters. This approach describes precipitation as the sum of a component from local evapotranspiration and another component from advected moisture, where the latter is treated as a known and constant model parameter. Setting advection to a constant value is not a desirable construction in our case where precisely the free interaction between land and ocean through advection is of interest.~~ Instead, we ~~use the empirical parametrization of~~ precipitation as a function mean water vapor pass, w, introduced by Bretherton et al. (2004). ~~They find that the precipitation rate over tropical oceanic regions shows an exponential relationship with w,~~

$$P(w) = \exp\left[a\left(\frac{w}{w_\mathrm{sat}} - b\right)\right]. \tag{6}$$

Equation (6) introduces two dimensionless parameters a and b and the saturated water vapor pass w_sat in mm. ~~Lacking a corresponding expression for extratropical ocean regions and land in general, we make the explicit assumption that Eqn. (6) holds everywhere and that the three parameters are the same over ocean and land. This assumption is rather crude and has major implications for the results presented in Section 4 as will be discussed in greater detail later on.~~

The qualitative dependence of evapotranspiration E_ℓ on soil moisture saturation is long-known, see e.g. Budyko (1956) ~~or more recently and slightly modified in Seneviratne et al. (2010).~~ E_ℓ is close to zero for soil moisture saturation values below the permanent wilting point, $s < s_\mathrm{pwp}$, increases approximately linearly in a transition range between the permanent wilting point and a

critical value close to the field capacity, $s_{\mathrm{pwp}} < s < s_{\mathrm{fc}}$, and reaches a plateau for higher s-values, $s > s_{\mathrm{fc}}$, where evapotranspiration is nearly constant. ~~The plateau value is denoted by potential evapotranspiration E_{p}, an energy-dependent parameter that increases with increasing radiative energy input. In this work, we assume constant energetic conditions E_{p} is set to a fixed value.~~ For computational convenience, we parametrize evapotranspiration by the following smooth function which has the qualitative properties described above,

$$E_\ell(s) = \frac{E_{\mathrm{p}}}{2}\left[\tanh\left(10\left(s - \frac{s_{\mathrm{pwp}} + s_{\mathrm{fc}}}{2}\right)\right) + 1\right]. \tag{7}$$

~~Equation (7) implies that the entire land box is either covered by a single vegetation type or that a combination of vegetation types can be modelled by means of an effective mean value of s_{pwp}, s_{fc} and E_{p}.~~ Unlike the land, the ocean is always fully saturated and we assume the resulting ocean evaporation rate E_{o} to be a constant model parameter.

It remains to find expressions for the *mean net* advection rates into the land and ocean atmospheres, hereafter just land/ocean advection rates. The total net advection into a given box is the difference between the moisture entering and leaving the box per unit time which is computed from the windward and leeward boundary water vapor pass values, w_{in} and w_{out}, respectively, multiplied by the mean horizontal background wind velocity u in m/s (and converted mm/day when used in computations). ~~The total amount of advected moisture in mm^2/day can then be expressed as~~

$$A_{\mathrm{tot}} = (w_{\mathrm{in}} - w_{\mathrm{out}})u. \tag{8}$$

The assumed water vapour pass distribution is characterized by one value w_{o} across the ocean atmosphere and another value w_ℓ across the land atmosphere. Hence, wind transports the moisture amount $w_{\mathrm{o}}u$ into the land domain and $w_\ell u$ into the ocean domain. ~~Since we only have two boxes and periodic boundary conditions, the total net advection rates, $A_{\mathrm{tot,l}}$ and $A_{\mathrm{tot,o}}$, into the land and ocean domains, respectively, are identical in magnitude but with opposite signs.~~ Translating this total advection rate into mean advection rates *per unit length* in mm/day gives

$$A_\ell = \frac{(w_{\mathrm{o}} - w_\ell)u}{\alpha L} = \frac{(w_{\mathrm{o}} - w_\ell)}{\alpha}\tau \tag{9}$$

TABLE 1. Parameter ranges for closed model simulations with uniform random sampling of parameter values.

Parameter	Minimum	Maximum	Range choice motivated by
s_{pwp}	0.20	0.55	Hagemann and Stacke (2015)
s_{fc}	0.50	0.85	Hagemann and Stacke (2015), assuming $s_{\mathrm{fc}} = s_{\mathrm{pwp}} + 0.3$
e_{p} [mm/day]	2.0	6.0	Rodriguez-Iturbe et al. (1991)
nZr [mm]	50.0	120.0	Rodriguez-Iturbe et al. (1991)
e_{o} [mm/day]	2.8	3.2	C. Hohenegger, private communications
ϵ	0.9	1.1	Rodriguez-Iturbe et al. (1991)
r	2	6	Rodriguez-Iturbe et al. (1991), Entekhabi et al. (1992)
a	11.4	15.6	Bretherton et al. (2004)
b	0.5	0.6	Bretherton et al. (2004)
w_{sat} [mm]	65.0	80.0	Bretherton et al. (2004)
α	0.0	1.0	full possible range
u [m/s]	1.0	10.0	lower tropospheric mean wind speeds
L [km]	1000.0	40000.0	chosen to represent different length scales
$\tau = u/L$ [day^{-1}]	0.00216	0.864	computed from extreme L and u
τ^{-1} [day]	1.16	462.96	computed from extreme L and u

for land advection and

$$A_{\mathrm{o}} = -\frac{(w_{\mathrm{o}} - w_{\ell})u}{(1-\alpha)L} = -\frac{(w_{\mathrm{o}} - w_{\ell})}{(1-\alpha)}\tau, \tag{10}$$

for ocean advection. On the right hand sides of Eqns. (9) and (10), we introduced the atmospheric transport parameter $\tau = u/L$ in days^{-1}. Its inverse value τ^{-1} represents a characteristic timescale for atmospheric transport. Multiplied by the land and ocean fraction, respectively, $\alpha\tau^{-1}$ and $(1-\alpha)\tau^{-1}$ correspond to the transport parameter χ used by Brubaker et al. (1991) as a control parameter for the "rate of moisture exchange between the oceanic and continental boxes" ~~(a~~ similar concept is used by Sobel and Bellon (2009) and Lintner et al. (2013) to model advection~~)~~. The range of χ values determined by Brubaker et al. (1991) from observations for a domain with $\alpha \approx 0.5$ is consistent with the τ^{-1} values that arise from the ranges of values for u and L used in this study. ~~The chosen ranges for all 12 model parameters are provided in Table 1. These ranges are used to construct the parameter space throughout which we constrain the precipitation partitioning and test the sensitivity of the model results to parameter variations.~~

3. Evaluation methods

In this section, we present the different analysis methods that are employed to evaluate the model behavior and to assess the sensitivity of the precipitation partitioning to a variation of the model parameters. The partitioning is quantified by the precipitation ratio,

$$PR = \frac{P_\ell}{P_\mathrm{o}} = \frac{P(w_\ell)}{P(w_\mathrm{o})}. \tag{11}$$

Since the moisture state of Earth's land-ocean-atmosphere system can be described as a steady state on sufficiently long timescales, we want to compute PR from the equilibrium values of w_ℓ and w_o. The equilibrium solution to the model equations (1) to (3) has to be found numerically. We use the DynamicalSystems.jl library from Datseris (2018) to find all roots of the model equations and determine whether each root represents a stable or unstable fixed point of the system.

Adopting an agnostic view on the plausibility of different combinations of parameter values from the ranges given in Table 1, we are confronted with a 12-dimensional parameter space with uniform probability distribution. ~~A general assessment of the sensitivity of equilibrium states and related quantities to a variation of the model parameters requires a sampling of the full parameter space~~. To this end, we perform $n = 50000$ model simulations for randomly chosen combinations of parameter values, each yielding a corresponding fixed point.

~~Having obtained a dataset of parameter values and corresponding equilibrium solutions in this way, the sensitivity of a computed quantity Q to each of the twelve parameters p_i can be visually and quantitatively evaluated with Q-p_i scatter plots.~~ For a potentially non-linear and non-monotonic distribution of the data points, a suitable ~~sensitivity~~ measure is the mutual information $MI(p_i, Q)$ ~~which~~ quantifies how much knowing the value of p_i will reduce the uncertainty about Q. Mutual information MI is computed as,

$$MI(p, Q) = H(p) + H(Q) - H(p, Q), \tag{12}$$

where $H(p_i)$, $H(Q)$ and $H(p_i, Q)$ are the information entropies [Shannon (1948)] of p_i and Q values and their joint distribution, respectively~~, where~~ we use amplitude binning to ascribe probability distributions. We follow ~~an~~ approach from Datseris and Parlitz (2022) ~~that computes~~

the significance level of an obtained sensitivity value ~~and compares the sensitivity of the different parameters. As a measure of the significance level, we define~~ the mutual information index

$$I_{MI}(p_i) = \frac{MI(\hat{p}_i, Q)}{MI_{\text{uncorr},3\sigma}(\hat{p}_i, Q)}, \tag{13}$$

where $\hat{p}_i$ denotes a version of p_i for which values have been rescaled to range between 0 and 1. $MI_{\text{uncorr},3\sigma}(\hat{p}_i, Q)$ is the mutual information value that deviates by three standard deviations σ from the mean of a distribution of MI values that is generated from shuffled surrogates of $\hat{p}_i$ and Q, representing the null-hypothesis of uncorrelated $\hat{p}_i$ and Q. A detailed description of this method is presented in Appendix [***]. $I_{MI} = 1$ is used as the significance threshold. The higher $I_{MI}(p_i)$, the more sensitive Q is to a variation of parameter p_i.

4. Basic model behavior and implications for PR

The results presented in this section are based on the data of 50000 simulations of the closed model introduced in Section 2 which randomly sample the parameter space as explained in Section 3. This data is henceforth referred to as "CM data". Each simulation yields the equilibrium solution for a unique point in the parameter space provided in Table 1.

Figure 2 shows the probability density functions (PDF) of equilibrium soil moisture (left and middle panel) and water vapor pass values for land and ocean atmospheres (right panel). In the middle panel, s is rescaled to $\tilde{s} = (s - s_{\text{pwp}})/(s_{\text{fc}} - s_{\text{pwp}})$ in order to demonstrate the relative location of the equilibrium values in the different regimes of evapotranspiration, E_ℓ~~, described in Section 2b. Values between the two dotted vertical lines fall into the transition regime between permanent wilting point and field capacity, in which evapotranspiration is water limited and increases strongly with s.~~ The bulk of all simulations equilibrates to intermediate soil moisture values between $s = 0.25$ and 0.75 with a sharp peak in the center part of the E_ℓ-transition regime around $\tilde{s} = 0.5$. Similarly, the atmospheres equilibrate to intermediate w_{o} and w_ℓ values between 40 and 50 mm, well below the saturation water vapor pass values given in Tab. 1. I could quantify the relative humidity here. Should I? ~~The moisture distribution for the land atmosphere is slightly shifted towards lower values, reflecting drier conditions over land than over ocean.~~ Only few simulations result in very dry or moist soil moisture and atmospheric states. We will come back to these cases when discussing parameter sensitivities.

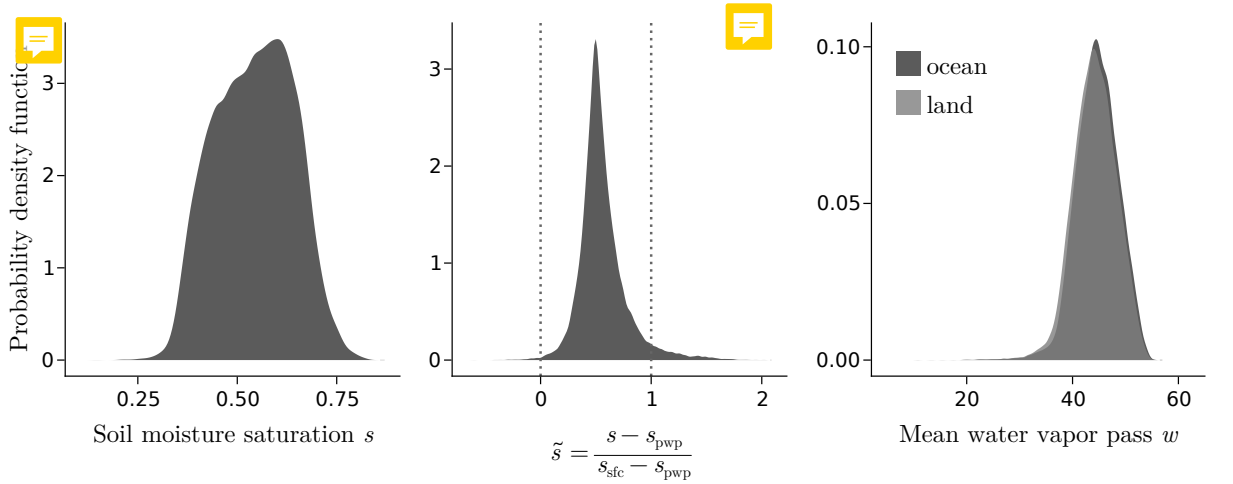

FIG. 2. Probability density functions of equilibrium soil moisture values (left panel), rescaled soil moisture values with vertical lines denoting the beginning and end of the transition regime of E_ℓ (middle panel), and mean water vapor pass of the land and ocean atmospheres (right panel).

Figure 3 shows rolling averages of the equilibrium flux rates from all simulations as functions of the equilibrium soil moisture saturation values s. ~~The displayed average flux rates are land precipitation P_ℓ, ocean precipitation P_o, ocean evaporation E_o, land evapotranspiration E_ℓ, runoff R and land and ocean advection, A_ℓ and A_o, respectively.~~ Note that the ocean advection rate A_o has negative values for all equilibrium solutions and is therefore multiplied by -1 to simplify the comparison of its magnitude with other fluxes. Figure 3 contains the entire CM data, i.e. solutions for all different combinations of parameter values. Therefore, one should not confuse the plotted curves with well-defined ~~functions of s with fixed parameter values~~. ~~For instance, the flattening of E_ℓ (geen line) beyond $s \approx 0.35$ is unrelated to the plateau regime of the E_ℓ-parametrization of Eqn. (7) above the field capacity. We already concluded from the PDF of $\tilde{s}$ in Fig. 2 that most equilibrium soil moisture values lie in the transitional E_ℓ-regime and that the plateau regime is hardly ever attained. The shape of E_ℓ in Fig. 3 is therefore a result of averaging over equilibrium points on different realisations of Eqn. (7) corresponding to different combinations of s_pwp, s_fc and E_p values.~~

~~Even though we cannot readily understand the diverse interplay of different parameter choices that shapes the lines in Figure 3, three qualitative observations allow for drawing first~~ conclusions about the partitioning of precipitation in the modelled land-ocean-atmosphere system:

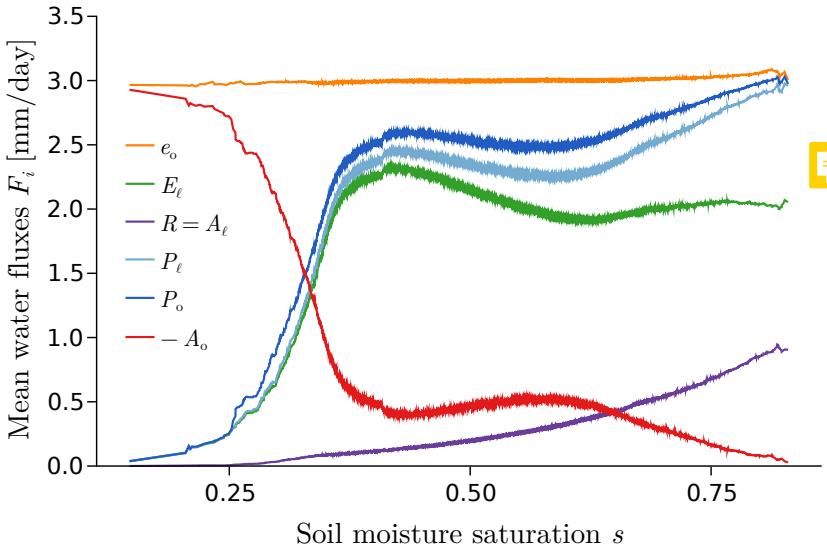

FIG. 3. Symmetric rolling average of equilibrium fluxes versus soil moisture saturation computed from CM data. For evapotranspiration (green line), the individual data points are shown as scatter plots and the range of $E_\ell(s)$ parametrizations for different parameter combinations is shaded in light green.

1. Land advection, A_ℓ (purple line) is strictly positive, meaning that moisture is always supplied by the ocean atmosphere to the land atmosphere. This net advection to the land compensates for the soil's constant loss of water through runoff, i.e. $A_\ell = R$. This compensation mechanism in equilibrated hydrological cycles has been described in earlier studies, e.g. by Horton (1943) or Peixóto and Oort (1983).

2. According to the advection equations (9) and (10), ~~the~~ net water transport from ocean to land requires the ocean atmosphere to be moister than the land atmosphere, $w_o > w_\ell$. Since the same, monotonically increasing function ~~$P(w)$~~ ~~from Eqn. (6)~~ is used for land and ocean ~~precipitation alike~~, $P_o = P(w_o)$ is necessarily larger than $P_\ell = P(w_\ell)$. In other words, mean precipitation is always stronger over ocean than over land. This is confirmed by Fig. 3 where the dark blue curve for P_o always lies above the bright blue curve for P_ℓ. ~~As a direct consequence, the precipitation ratio is bound by an upper limit of one, i.e.~~ ~~$PR = P_\ell/P_o < 1$.~~

3. The ocean evaporation rate E_o (orange line) is always the largest ~~flux, i.e. all other fluxes lie within the open interval $(0, E_o)$~~. This can be explained as follows: e_o is partitioned into ocean precipitation P_o and ocean advection $|A_o|$ so that each of the two components needs to be

smaller than e_o. Since the land atmosphere is drier than the ocean atmosphere, it follows that $P_\ell < P_o < e_o$. Land precipitation can be written as the sum of ~~fluxes,~~ $\cancel{P_\ell = E_\ell + R = E_\ell + A_\ell}$, so that again, each of these components needs to be smaller than e_o.

The ~~shapes of the lines in Figure 3 indicate that three soil moisture regimes can be distinguished:~~ For low soil moisture values up to $s \approx 0.4$, runoff and advection are negligible and precipitation ~~follows the shape of~~ $\cancel{E_\ell}$. In an intermediate soil moisture regime, $0.4 \lesssim s \lesssim 0.6$, precipitation flattens due to a balancing effect of decreasing evapotranspiration and increasing advection. Lastly, above $s \approx 0.63$, $\cancel{E_\ell}$ ~~remains nearly constant. Increasing runoff and advection dominate this regime and lead to a rise in precipitation. Understanding these regimes requires a deeper insight into parameter sensitivities and how different parameters interact. For instance, we will see that low~~ $\cancel{s}$ ~~values are only attained when the land fraction is sufficiently large and that high~~ $\cancel{s}$ ~~values require a high permanent wilting point as well as efficient atmospheric transport. Such considerations will also resolve the~~ apparent contradiction of an overall declining moisture advection from the ocean atmosphere (red line) while the advection into the land atmosphere (purple line) is monotonically increasing over the range of s.

5. Parameter sensitivity of PR

We measure the relative parameter sensitivity of the precipitation ratio by the mutual information index $I_{MI}(p_i)$ defined in Eqn. (13). A comparison of the results for all model parameters p_i is provided in Figure 4. ~~The significance threshold,~~ $\cancel{I_{MI} = 1}$~~, is marked by the dashed line (see Section 3 and Appendix [XXX] for details).~~ The atmospheric transport parameter τ is by far the most sensitive parameter, followed by land fraction α and the three soil parameters permanent wilting point s_{pwp}, field capacity s_{fc}, and runoff parameter r. Note that we coupled the field capacity value to the permanent wilting point by $s_{\mathrm{fc}} = s_{\mathrm{pwp}} + 0.3$, so that the two can be treated together in the following discussion of physical mechanisms for the different sensitivities. Some of the remaining parameters, most notably potential evaporation E_{p}, also have I_{MI}-values above or close to the significance threshold but we do not discuss them in detail due to their rather small contributions to the overall sensitivity.

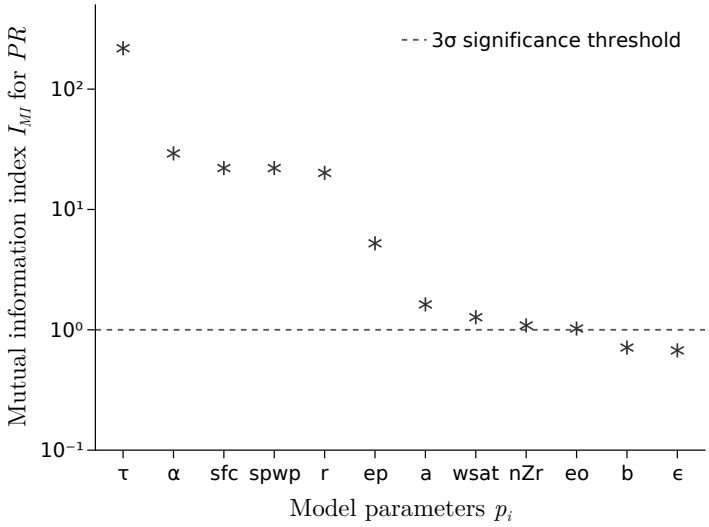

FIG. 4. Relative sensitivity of the precipitation ratio to the variation of different model parameters p_i measured by the mutual information index I_{MI}. Values larger than $I_{MI} = 1$ (dashed line) lie above the significance threshold.

a. Atmospheric transport parameter τ

Figure 5 shows scatter plots of the precipitation ratio versus the four most sensitive model parameters. The relationship between PR and τ (top left panel) is strongly nonlinear and ~~very distinct~~, confirming the high sensitivity determined in the mutual information analysis. The precipitation ratio is low for low values of τ and converges towards one as τ increases. The spread of PR values around the mean (dark grey line) decreases along increasing τ, making τ a better predictor for the precipitation partitioning as its value increases.

Physically, τ corresponds to the fraction of the total domain length that moisture can travel horizontally in the atmosphere in one day. As such, it can be interpreted as an efficiency of atmospheric moisture transport ~~and has direct implications for the ability of advection to assimilate the moisture conditions over land and ocean~~. High values of τ imply a fast exchange of moisture between land and ocean atmospheres with the result of relatively low moisture differences, $\Delta w = w_o - w_\ell$. Since we assume the same precipitation parametrization $P(w)$ for land and ocean, ~~Δw represents a proxy for PR. Small values of Δw mean similar moisture conditions in the two atmospheres with similar rain rates~~ and PR close to one. In contrast, small values of τ can sustain larger moisture differences and lead to smaller values for PR.

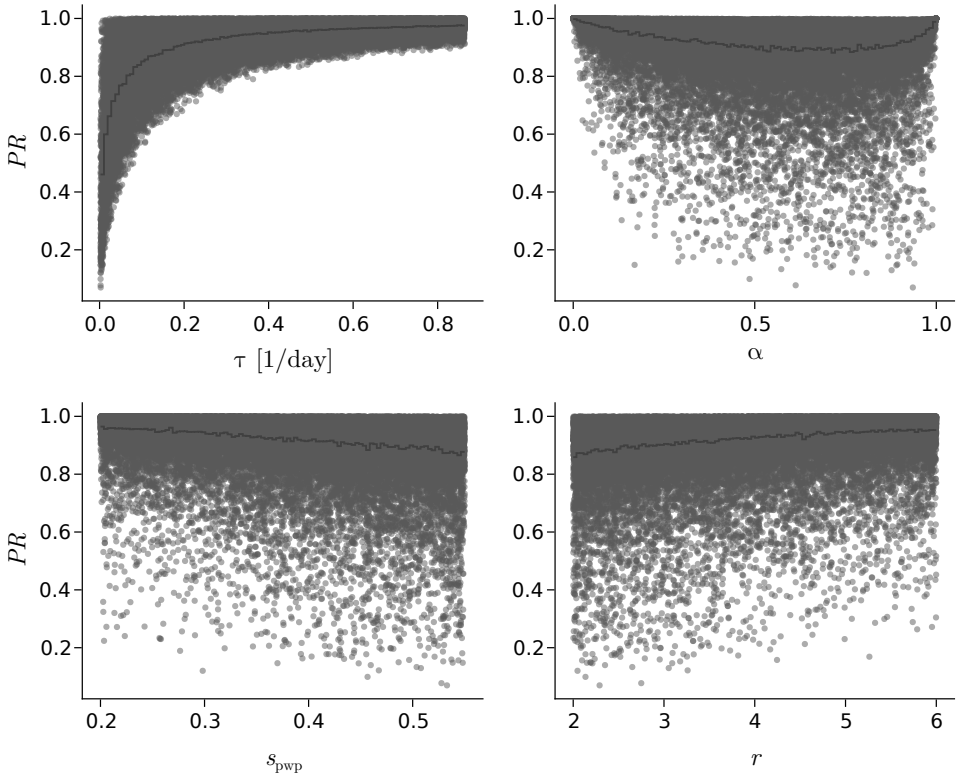

FIG. 5. Precipitation ratio versus atmospheric transport parameter τ, land fraction α, permanent wilting point s_{pwp} and runoff parameter r. The dark grey lines show means of bins of neighbouring parameter values.

However, the efficiency of advection does not solely rest on τ. It also depends on the land fraction and can be expressed as $\epsilon_{\mathrm{a},\ell} = \tau/\alpha$ in the case of land advection and as $\epsilon_{\mathrm{a,o}} = \tau/(1-\alpha)$ in the case of ocean advection. In this way, we may rephrase Eqns. (9) and (10) as products of moisture difference Δw and parametric efficiencies $\epsilon_{\mathrm{a},\ell}$ and $\epsilon_{\mathrm{a,o}}$, respectively. Since α ranges between zero and one, it is the value of τ that sets the lower bound of the efficiency and, hence, the minimum of PR. This role of τ also becomes clear in Fig. 5 (top left) where the lower bound of PR values increases with τ.

b. Land fraction α

The role of α in the advection efficiencies is to differentiate between the efficiency of moisture export out the ocean domain and the efficiency of moisture import into the land domain. If α is small, the average time for moisture from the large ocean surface to reach the land is long,

making the ocean advection inefficient (low $\epsilon_{a,o}$). In contrast, it takes only little time to distribute the imported moisture over the small land size so that land advection is efficient (high $\epsilon_{a,\ell}$). The reverse applies for a large land fraction.

Fig. 5 (top right panel) illustrates how α impacts the partitioning of precipitation. The mean ~~value of PR~~ forms a u-shaped line between the extreme cases of an ocean-only, $\alpha = 0$, and land-only, $\alpha = 1$, scenario where in both cases atmospheric conditions over land and ocean are approximately the same and PR is close to one. While the model cannot handle the exact endpoints of the α-range, we can examine them in a thought experiment: Imagine a domain fully covered by ocean. Water balance would require the ocean precipitation to exactly balance ocean evaporation, $P_o = E_o$. If we now introduced an infinitesimal patch of land, some of the evaporated moisture would be advected into the tiny land atmosphere. Since $\epsilon_{a,\ell}$ is high, the atmospheric conditions would assimilate rapidly without significantly altering the moisture conditions over the vast ocean. Hence, for such small α, the system is expected to behave as if the land didn't exist ~~with moist atmospheric conditions and precipitation rates~~ $\cancel{P_\ell \lesssim P_o \lesssim E_o}$. ~~As~~ the other extreme case, imagine a pure land domain but with the assumption that runoff remains possible. The runoff would continuously reduce the soil moisture saturation and with it evapotranspiration and precipitation until the trivial equilibrium solution $\{s = 0, w_\ell = 0\}$ ~~was~~ reached. Allowing for advection from an infinitesimal ocean would not change the picture much. With very high efficiency $\epsilon_{a,o}$, almost the entire but nevertheless small amount of oceanic moisture, $\cancel{(1-\alpha)LE_o \gtrsim 0}$, would be exported to the land, leaving behind a fairly dry ocean atmosphere and hardly affecting the dry moisture state of the large land atmosphere and soil. Hence, we expect a situation in which the system behaves as if the ocean didn't exist with precipitation rates $\cancel{P_o \gtrsim P_\ell \gtrsim 0}$.

The behavior of the individual rain rates, P_o and P_ℓ, over the range of α is shown in Figure 6 and confirms the developed arguments. ~~Overall moist conditions prevail for low α and dry conditions for high α with a regime of monotonic drying inbetween~~. Expressions for the rain rates can be found by imposing equilibrium conditions, ~~i.e. vanishing time derivatives~~, on Eqns. (2) and (3),

$$P_\ell = E_\ell(s(\alpha)) + \Delta w(\alpha)\epsilon_{a,\ell}(\alpha) \tag{14}$$

$$P_o = e_o - \Delta w(\alpha)\epsilon_{a,o}(\alpha). \tag{15}$$

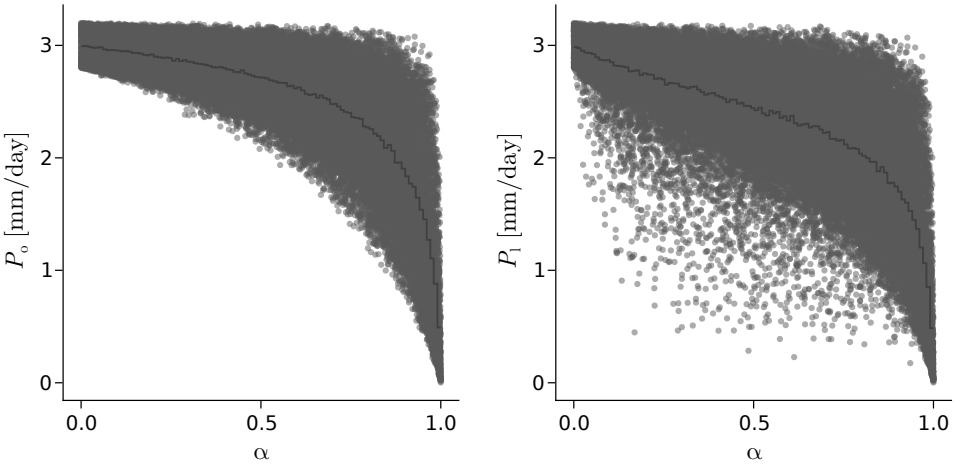

FIG. 6. Ocean precipitation rate P_o and land precipitation rate P_ℓ versus land fraction α. The transition from an ocean-only to a land-only model scenario is marked by a decrease of both precipitation fluxes, indicating overall moist conditions for small and dry conditions for large land fractions.

Note that we know the shapes of $\epsilon_{a,\ell}(\alpha)$ and $\epsilon_{a,o}(\alpha)$ while the $s(\alpha)$ and $\Delta w(\alpha)$ are implicit but not analytical functions of the land fraction. As α increases in Fig. 6, P_ℓ decreases more strongly than P_o because land precipitation is not only affected by (initially sharply) decreasing $\epsilon_{a,\ell}$ but in addition by a reduction in evapotranspiration as s declines. In contrast, ocean precipitation is only reduced by (initially weakly) increasing advection. In Figure 5 (top right), these different shapes of land and ocean precipitation manifest in the asymmetry of the $PR(\alpha)$ mean values (dark grey line) with a minimum around $\alpha = 0.75$, ~~representing the largest moisture difference between the two atmospheres. However, the spread of PR values around the mean is considerable for intermediate values α and the location of the minimum is different for each combination of the other parameter values.~~ Generally, the ~~shape~~ of the spread indicates that the land fraction is the dominant predictor for PR near its extreme values but that it loses much of its predictive power for intermediate values.

c. *Permanent wilting point s_{pwp} and field capacity s_{fc}*

Different soil types are characterised by different permanent wilting points and field capacities. For instance, $s_{pwp} \approx 0.3$ might correspond to loam and $s_{pwp} \approx 0.5$ to clay (Hagemann and Stacke (2015)). The left panel of Figure 7 displays how a change of s_{pwp}, and with it s_{fc}, corresponds to a shift of the evapotranspiration function along s while its shape remains unchanged. In the

evapotranspiration graphs, s_{pwp} determines the soil moisture value at which the curve transitions from $E_\ell \approx 0$ to the regime of steeply increasing E_ℓ and s_{fc} marks the beginning of the plateau on which E_ℓ saturates for high s.

~~In the bottom right panel of Figure 5, we see a negative trend of the precipitation ratio with increasing s_{pwp}.~~ To understand this trend, it is convenient to think of a system in equilibrium for some permanent wilting point, e.g. $s_{\mathrm{pwp}} = 0.3$. The mean equilibrium soil moisture value in the CM data for $s_{\mathrm{pwp}} = 0.3$ is $s = 0.43$. This initial state of the model is displayed as a blue dot in Figure 7. An abrupt increase of the permanent wilting point to $s_{\mathrm{pwp}} = 0.4$ leads to an instantaneous drop ΔE_{inst} in the evapotranspiration as illustrated by the first red arrow connecting the blue and green dot in the left panel of Fig. 7. The green dot represents a temporary state where the model is not in equilibrium because the state variables have not yet been adjusted to the new situation. At this point, the soil receives the same amount of precipitation but loses less water through evapotranspiration. As a result, the soil moistens. As time progresses, the system attains a new equilibrium state at a higher s value which is marked by the orange dot. This moistening of the soil is shown in the right panel of Fig. 7, where the equilibrium s values of the CM data are plotted over the corresponding values of s_{pwp}. However, as the soil moistens, runoff and land advection increase, too. Assuming that $\epsilon_{\mathrm{a},\ell}$ is kept fixed, Δw has to increase to ~~facilitate~~ the increase of advection. The water that is advected to the land atmosphere is taken from the ocean atmosphere, where w_{o} decreases as a consequence. Hence, an increase in advection is only possible, if w_ℓ decreases more strongly than w_{o}. As a decrease in w_ℓ reduces P_ℓ, the new equilibrium is characterised by weaker precipitation ~~which needs to provide water for increased runoff, leaving less water to evapotranspiration~~. Therefore, the attained equilibrium state for $s_{\mathrm{pwp}} = 0.4$ has a moister soil but an evapotranspiration rate which is by ΔE_{eq} lower compared to the initial state for $s_{\mathrm{pwp}} = 0.3$. The fact that w_ℓ must decrease more strongly than w_{o} in the adaptation process is the reason why PR declines with increasing s_{pwp} and s_{fc}.

d. Runoff parameter r

The relationship between PR and runoff parameter r in the bottom right panel of Figure 5 resembles the relationship of $PR(s_{\mathrm{pwp}})$ but with opposite trend: PR increases with r while it

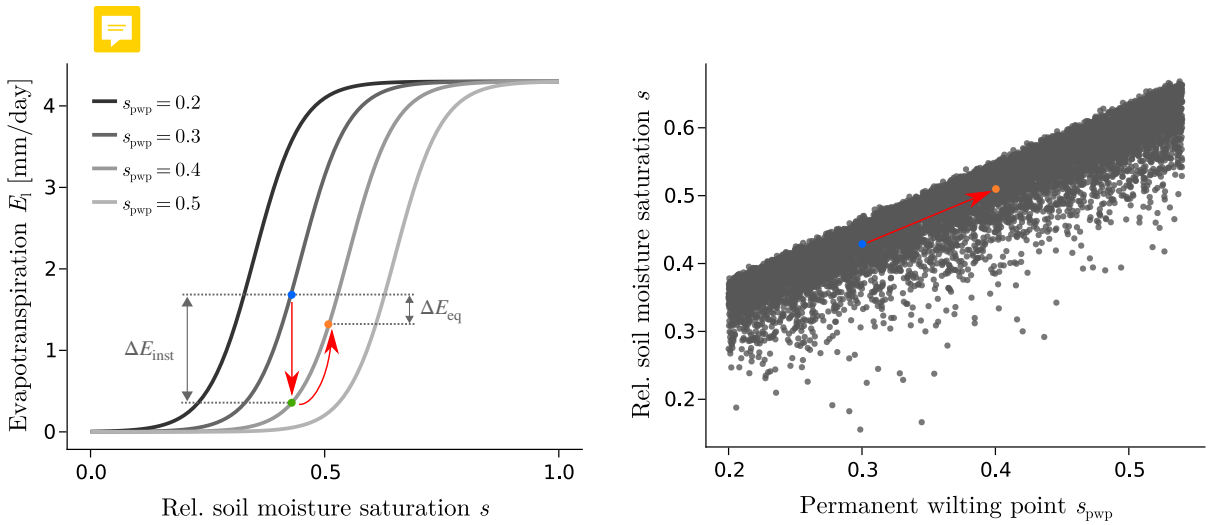

FIG. 7. Influence of an increase in s_{pwp} on the equilibrium state. Left: Higher values of s_{pwp} shift the graph of the E_ℓ parametrization towards larger s. Right: Equilibrium values of the soil moisture saturation from CM data plotted over s_{pwp} values.

decreases with s_{pwp}. Indeed, the similarity originates from a physical mechanism similar to the one discussed for the permanent wilting point.

In the formulation of the runoff fraction, $R_f = \epsilon s^r$, r enters as the exponent. ~~Assuming a constant ϵ = 1.0, all realisations of R_f are zero for s = 0 and one for s = 1. The path on which R_f gets from zero to one as s increases is determined by r. Higher values for r delay the increase of runoff and steepen the slope of the increase at higher s. At any given soil moisture value, higher r results in lower R_f.~~

As in the discussion of the s_{pwp}-dependence, we can think of an equilibrium state but this time suddenly increase the value of r. As a consequence, runoff drops to a lower value and soil moisture begins to increase. As a response, also both atmospheres start to moisten: First, w_l moistens through increased evapotranspiration from the wetter soil, reducing the moisture difference between land and ocean. Second, the reduction of Δw implies reduced advection, allowing the ocean atmosphere to keep more of its moisture to itself, and w_o increases. At some point, the decreasing advection matches the runoff which started to intensify again after the initial drop as the soil moistened. A new equilibrium is attained in which runoff is ~~overall~~ reduced compared to the initial state that had a ~~higher~~ r-value. The equally reduced land advection with lower Δw reflect assimilated atmospheric moisture conditions and, hence, increased PR.

6. Under which circumstances can PR become larger than 1?

So far, we established that the precipitation ratio is constrained to an upper limit of one due to the necessity of net moisture transport from ocean to land and the ~~assumption~~ that a moister atmosphere yields a higher precipitation flux. However, in the real world, local systems have been identified for which higher rain rates are observed over land compared to the surrounding ocean. For instance, Qian (2008), Sobel et al. (2011), and Ulrich and Bellon (2019) found precipitation enhancement over tropical islands and attributed this observation mainly to the development of sea breezes triggering precipitating convection over the islands. ~~Island size, orography and background wind speed were identified as additional factors contributing to the existence and magnitude of precipitation enhancement. Simulation studies such as Cronin et al. (2015) and Wang and Sobel (2017) confirm and further explain these underlying mechanisms.~~ We wonder if there are pathways through which precipitation enhancement over land can occur within our water balance framework.

a. Relaxing assumptions of the ~~conceptual~~ model

~~The result that $PR < 1$ is a consequence of a number of assumptions governing the conceptual model. Three of these assumptions seem particularly relevant in the context of precipitation enhancement.~~

~~First, we generalize that the empirical relationship between precipitation and integrated water vapor pass $P(w)$ for tropical oceans holds across the entire model domain, including the land.~~ While the qualitative statement that a moister atmosphere yields more rainfall seems robust, the exact shape of this relationship might differ over land and ocean ~~and in the tropics compared to higher latitudes~~. If different parametrizations $P_\ell(w)$ and $P_\mathrm{o}(w)$ were used for land and ocean precipitation, respectively, and $P_\ell(w)$ was larger than $P_\mathrm{o}(w)$ in the relevant range of w-values, it is conceivable that an equilibrium state could exhibit a moister ocean atmosphere ~~facilitating~~ net advection to the land and at the same time stronger land precipitation, so that $PR > 1$. The observational study by Bergemann and Jakob (2016) finds that tropical rainfall over land associated with coastal effects such as sea breezes can occur under drier atmospheric conditions than rainfall over the open ocean. On the other hand, they suggest that rainfall over coastal land without a direct link to coastal effects requires moister atmospheric conditions than over the open ocean. How

the shape of $P(w)$ over land differs from tropical oceanic regions ~~and to which degree the ocean parametrization by Bretherton et al. (2004) holds in extratropical regions~~ remain open questions.

Second, we treat the four model boxes as being homogeneous and well-mixed which allows us to work with mean fluxes rather than resolving the horizontal direction $\vec{x}$ explicitly. It is well-known that an airstream traversing an oceanic region will moisten along its trajectory since mean ocean evaporation typically exceeds mean ocean precipitation and the reverse is true for land regions ~~where precipitation dominates over evapotranspiration and the airstream loses moisture on its inland journey.~~ Ogino et al. (2016) and Ogino et al. (2017) further ~~find~~ that the conventional view in which Earth's surface gets divided into ocean and land misses out on particular interactions driven by the land-ocean contrast which are confined to a coastal region reaching a few hundred kilometers seaward and landward from the coast. These coastal regions receive higher amounts of precipitation than both the open ocean and inland continental regions. ~~Due to their relatively small spatial extent, islands are likely more affected by coastal precipitation mechanisms, with the result of increased mean precipitation compared to large continents or open oceans for which coastal effects are diminished when computing spatial averages. In our model, the coastal zone could, for example, be represented by its own box with a dedicated coastal precipitation parametrization $P_e(w)$.~~

Third, sea-breezes as the primary coastal process ~~impacting precipitation~~ are not captured by the presented model. In order to account for them, the model would need to be extended by a diurnal cycle - either fundamentally by coupling the water balance equations to energy balance equations, or indirectly by expressing ~~energy-dependent parameters such as τ,~~ E_o ~~and~~ E_p as time-dependent quantities that vary over the course of a day. Even with the same $P(w)$ for land and ocean, a diurnal cycle could make the mean precipitation ratio larger than one if the increased moisture transport from ocean to land during the day leads to higher temporary land precipitation rates than over the ocean and if the reverse transport during the night doesn't fully compensate for the daytime precipitation signal.

b. Open model for systems subject to synoptic-scale convergence/divergence

~~The presented conceptual model assumes that the described system is closed, meaning that net advection into or out of the model domain is zero. If we want to model small-scale systems such~~

~~as islands in isolation, this assumption is inapt and we should rather treat these objects and their surrounding ocean as an open system subject to large-scale divergence or convergence.~~ Moisture import or export from an external environment outside the model boundaries can be incorporated by an additional advection term, A_{ext} in mm/day in Equation (3) for the ocean atmospheric water balance. A positive A_{ext} denotes inflow of external moisture, while a negative A_{ext} means that the ocean atmosphere loses moisture through the model boundaries. Is this change in the model framework sufficient to create scenarios for which $PR > 1$?

We argue that the answer is no: Regardless of whether the system is gaining or losing moisture through its boundaries, an equilibrium state still requires a net transport of moisture from ocean to land, and therefore $w_{\text{o}} > w_\ell$ with $PR < 1$. The term A_{ext} acts in a similar fashion as ocean evaporation. Under the influence of moisture convergence, the positive A_{ext} is equivalent to an increase in E_{o} and merely increases the overall relative moisture saturation in all boxes. In the case of moisture divergence, negative A_{ext} acts as a reduction of E_{o} and an overall drier equilibrium state is attained as long as $|A_{\text{ext}}| < E_{\text{o}}$. If the loss through the model boundary is stronger than the moisture input from the ocean surface, the system will undergo drying until the trivial solution $\{w_{\text{o}} = 0, w_\ell = 0, s = 0\}$ is reached. ~~We show in the following that the conceptual step from a closed to an open model is nevertheless useful but that we have to explicitly resolve the spatial configuration of land and ocean with respect to the wind-driven airflow in order to see a qualitative effect on possible values for PR.~~

c. *Open model with resolved spatial configuration in flow direction*

~~In this section, we present simulation results for an open model~~ with a land box of length L_ℓ ~~which is~~ placed between two equally big ocean boxes ~~with~~ lengths $L_{\text{o1}} = L_{\text{o2}}$. All lengths are given in km. The subscript 'o1' refers to the ocean in front of the island as seen by an airflow horizontally traversing the model domain at constant wind speed, while 'o2' refers to the ocean behind the island. The model equations governing the evolution of the three mean atmospheric water vapor passes w_{o1}, w_ℓ and w_{o2} and soil saturation s are formulated in analogy to the closed model equations presented in Section 2 and can be found in Appendix [xxx] along with a model sketch. Note that this open model requires an additional parameter w_0 which represents the windward boundary water vapor pass and enters the advection term in the atmospheric equation for the first ocean. As

for the closed model, 50000 simulations with randomly chosen combinations of parameter values are performed, yielding a dataset of open model equilibrium solutions that we refer to as "OM data".

The precipitation ratio is now defined in terms of mean precipitation rates $\bar{P}_\ell$ and $\bar{P}_\mathrm{o}$ as

$$PR_\mathrm{om} = \frac{\bar{P}_\ell}{\bar{P}_\mathrm{o}} = \frac{2P_\ell}{P_\mathrm{o1} + P_\mathrm{o2}}. \tag{16}$$

As in the case of the closed model, equilibrium can only be attained if the land atmosphere receives advected moisture from the ocean. In the open model, this means that the first ocean atmosphere has to be moister than the land atmosphere which – sticking to the assumption of the same parametrization for precipitation across the model domain – implies $P_\mathrm{o1} > P_\ell$. It follows from Equation (16) that a precipitation ratio larger than one is possible if the second ocean atmosphere is dry enough to compensate for the relatively moist first ocean atmosphere and thereby reduces the mean ocean precipitation to a value smaller than P_ℓ. Mathematically, a precipitation ratio larger than one requires the inequality, $P_\mathrm{o2} < 2P_\ell - P_\mathrm{o1}$, to be fulfilled.

From the OM data, we find that only about 6.8 % of all simulations meet this condition and yield $PR_\mathrm{om} > 1$. These simulations have in common that atmospheric moisture reduces along the wind trajectory, i.e. $w_0 > w_\mathrm{o1} > w_\ell > w_\mathrm{o2}$. ~~They also show similarities in the values of the most sensitive parameters. The same sensitivity analysis as performed for the closed model (described in Section 3) reveals that~~ PR_om is most sensitive to w_0 and α, and ~~that~~ τ only appears in the third place. Figure 8 shows probability density functions (PDFs) over the possible values of w_0 ~~(left panel) and~~ $\cancel{\alpha}$ ~~(right panel)~~ for simulations with precipitation ratios smaller and larger than one in dark and light grey color, respectively. Even though the distributions have a significant overlap, $PR > \cancel{0}$ requires a large enough boundary water vapor pass $w_0 \gtrsim 40$ mm and becomes more likely with smaller land fraction. States with $PR > 1$ do not exist for $\alpha > 0.7$. This ~~is consistent with the PDFs for the equilibrium state variables (not shown) which identify simulations with~~ $\cancel{PR >}$ ~~1 as ones with overall moist conditions~~: The soil moisture saturation values cluster around values that correspond to the upper end of the transitional E_ℓ-regime and beyond the field capacity where E_ℓ reaches the plateau. Water vapor pass values peak around 50 mm ~~which corresponds to about 70 % relative humidity~~ and get no lower than 38 mm. Simulations with $PR < 1$ in contrast exhibit

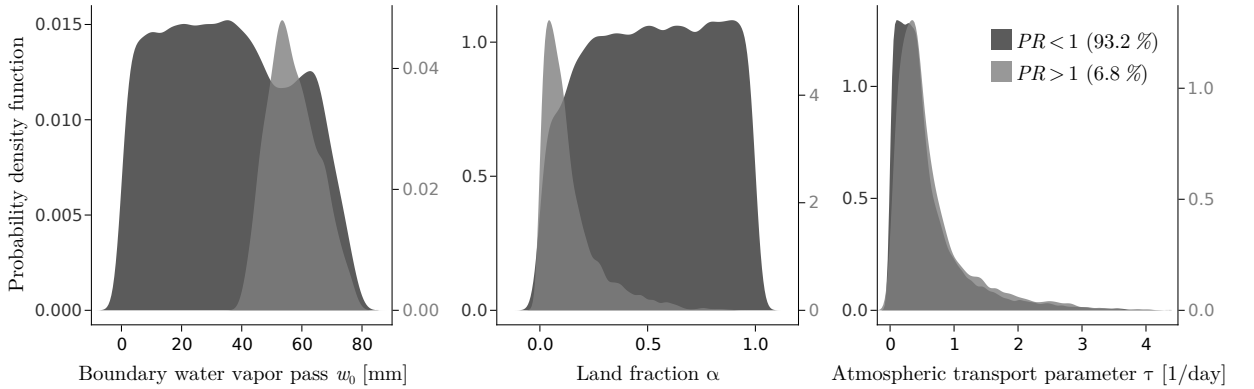

FIG. 8. Caption

equilibrium states across the entire moisture spectrum, including very dry states with soil moisture values below the permanent wilting point.

7. Conclusions

This study was motivated by our lack of theoretical understanding of how Earth's total precipitation gets partitioned between land and ocean. We wanted to know which ~~physical processes and quantities~~ determine the partitioning and what constraints can be set on the ratio between spatially averaged land and ocean precipitation rates, $PR = P_\ell / P_o$ based on water balance equations.

We introduced a conceptual box model that describes the rate of change of soil moisture and atmospheric moisture over ocean and land, respectively. The water balance components are expressed as known empirical parametric functions of the mean water content of the land and atmospheric boxes. In order to investigate the bounds of PR and its parameter sensitivity, we analyze a large number of equilibrium solutions for different combinations of model parameter values. The obtained results can be summarized as follows:

- ~~Since the fundamental property of soil to lose water through runoff to the ocean demands an equally large net atmospheric moisture transport from ocean to land, the ocean atmosphere in a closed, two-domain model configuration, equilibrates to a moister state than the land atmosphere. If the same relationship between precipitation and atmospheric moisture content holds for land and ocean regions, then the precipitation ratio is bound by an upper limit of $PR = 1$.~~

- ~~The lower bound of PR is mostly determined by the atmospheric transport parameter τ, which can be interpreted as the efficiency of atmospheric moisture transport. Efficient transport results in similar moisture conditions over land and ocean and, hence, similar precipitation rates, while~~ inefficient transport allows for larger moisture differences and an ocean precipitation up to ten times as strong as over land ($PR \approx 0.1$). ~~Significant sensitivity is also found for land fraction α and to a lesser extent to the permanent wilting point and field capacity of the soil. The land fraction is most relevant near its extreme values for a tiny land, $\alpha \longrightarrow 0$, where the overall moisture state of the model is wet and for a large land, $\alpha \longrightarrow 1$, where the moisture state is dry. In both extreme cases, the precipitation ratio attains values close to one, while for intermediate values, α loses much of its predictive power and the influence of τ dominates.~~

- The conceptual water balance model ~~has difficulties explaining~~ observed island precipitation enhancement as reported by other studies. ~~In the closed model configuration, PR-values larger than one could be obtained through different precipitation parametrizations over land and ocean, the implementation of energy balance equations or a diurnal cycle in the form of time-dependent parameters, and, possibly, through a more realistic land distribution. An alternative is an open model formulation of an island between two ocean boxes with a well-defined atmospheric flow direction and prescribed upstream boundary water vapor pass. This open formulation is more apt for simulating small scale systems since~~ net advection into or out of the domain ~~is permitted. However, this model is still subject to the same limiting assumptions of parametrization choices and constant energetic conditions.~~ We find precipitation enhancement over land compared to the mean precipitation of the surrounding ocean for a small subset of the performed open model simulations. These cases ~~are characterized by rather large water vapor pass boundary values and small land sizes.~~

Even though the simple conceptual model does not capture the full range of physical processes that influence the precipitation partitioning between land and ocean, it is able to constrain the precipitation ratio ~~to values close to observational estimates.~~ It identifies the efficiency of atmospheric transport as the dominant factor governing the partitioning, while soil parameters are shown to be less influential.

Acknowledgments.

Data availability statement.

References

Bergemann, M., and C. Jakob, 2016: How important is tropospheric humidity for coastal rainfall in the tropics? *Geophysical Research Letters*, **43 (11)**, 5860–5868, https://doi.org/10.1002/2016GL069255, URL https://onlinelibrary.wiley.com/doi/abs/10.1002/2016GL069255.

Bretherton, C. S., M. E. Peters, and L. E. Back, 2004: Relationships between water vapor path and precipitation over the tropical oceans. *J. Climate*, **17**, 1517–1528, https://doi.org/10.1175/1520-0442(2004)017<1517:RBWVPA>2.0.CO;2.

Brubaker, K., D. Entekhabi, and P. Eagleson, 1991: Atmospheric water vapor transport: Estimation of continental precipitation recycling and parameterization of a simple climate model. URL https://ntrs.nasa.gov/citations/19910018381.

Brubaker, K. L., D. Entekhabi, and P. S. Eagleson, 1993: Estimation of continental precipitation recycling. *Journal of Climate*, **6**, 1077–1089, https://doi.org/10.1175/1520-0442(1993)006<1077:EOCPR>2.0.CO;2, URL https://journals.ametsoc.org/jcli/article/6/6/1077/39303/Estimation-of-Continental-Precipitation-Recycling.

Budyko, M. I., 1956: *Heat balance of the Earth's surface*. U.S. Dept. of Commerce, Weather Bureau.

Budyko, M. I., and O. A. Drozdov, 1953: Characteristics of the moisture circulation in the atmosphere. **4**, 5–14.

Burde, G. I., and A. Zangvil, 2001: The estimation of regional precipitation recycling. part i: Review of recycling models. *Journal of Climate*, **14 (12)**, 2497–2508, https://doi.org/10.1175/1520-0442(2001)014<2497:TEORPR>2.0.CO;2, URL https://journals.ametsoc.org/jcli/article/14/12/2497/29526/The-Estimation-of-Regional-Precipitation-Recycling.

Cronin, T. W., K. A. Emanuel, and P. Molnar, 2015: Island precipitation enhancement and the diurnal cycle in radiative-convective equilibrium. **141 (689)**, 1017–1034, https://doi.org/10.1002/qj.2443, URL https://rmets.onlinelibrary.wiley.com/doi/abs/10.1002/qj.2443.

Datseris, G., 2018: Dynamicalsystems.jl: A julia software library for chaos and nonlinear dynamics. *Journal of Open Source Software*, **3**, 598, https://doi.org/10.21105/joss.00598.

Datseris, G., and U. Parlitz, 2022: *Nonlinear Dynamics*. 2192-4791, Springer International Publishing, URL https://link.springer.com/book/9783030910334.

Eltahir, E. a. B., and R. L. Bras, 1994: Precipitation recycling in the amazon basin. *Quarterly Journal of the Royal Meteorological Society*, **120**, 861–880, https://doi.org/10.1002/qj.49712051806, URL https://onlinelibrary.wiley.com/doi/abs/10.1002/qj.49712051806.

Ent, R. J. v. d., H. H. G. Savenije, B. Schaefli, and S. C. Steele-Dunne, 2010: Origin and fate of atmospheric moisture over continents. *Water Resources Research*, **46 (9)**, https://doi.org/10.1029/2010WR009127, URL https://agupubs.onlinelibrary.wiley.com/doi/abs/10.1029/2010WR009127.

Entekhabi, D., I. Rodriguez-Iturbe, and R. L. Bras, 1992: Variability in large-scale water balance with land surface-atmosphere interaction. *Journal of Climate*, **5**, 798–813, https://doi.org/10.1175/1520-0442(1992)005<0798:VILSWB>2.0.CO;2, URL https://journals.ametsoc.org/jcli/article/5/8/798/35919/Variability-in-Large-Scale-Water-Balance-with-Land.

Hagemann, S., and T. Stacke, 2015: Impact of the soil hydrology scheme on simulated soil moisture memory. *Climate Dyn.*, **44**, 1731–1750, https://doi.org/10.1007/s00382-014-2221-6.

Horton, R. e., 1943: Hydrologic interrelations between lands and oceans. *Eos, Transactions American Geophysical Union*, **24 (2)**, 753–764, https://doi.org/10.1029/TR024i002p00753, URL https://onlinelibrary.wiley.com/doi/abs/10.1029/TR024i002p00753.

Lintner, B. R., P. Gentine, K. L. Findell, F. D'Andrea, A. H. Sobel, and G. D. Salvucci, 2013: An idealized prototype for large-scale land–atmosphere coupling. *Journal of Climate*, **26 (7)**, 2379–2389, https://doi.org/10.1175/JCLI-D-11-00561.1, URL https://journals.ametsoc.org/view/journals/clim/26/7/jcli-d-11-00561.1.xml.

Ogino, S.-Y., M. D. Yamanaka, S. Mori, and J. Matsumoto, 2016: How much is the precipitation amount over the tropical coastal region? *Journal of Climate*, **29 (3)**, 1231–1236, https://doi.org/10.1175/JCLI-D-15-0484.1, URL https://journals.ametsoc.org/view/journals/clim/29/3/jcli-d-15-0484.1.xml.

Ogino, S.-Y., M. D. Yamanaka, S. Mori, and J. Matsumoto, 2017: Tropical coastal dehydrator in global atmospheric water circulation. *Geophysical Research Letters*, **44 (22)**, 11,636–11,643, https://doi.org/https://doi.org/10.1002/2017GL075760, URL https://agupubs.onlinelibrary.wiley.com/doi/abs/10.1002/2017GL075760%4010.1002/%28ISSN%291944-8007.GRLHIGHLIGHTS2017.

Peixóto, J. P., and A. H. Oort, 1983: The atmospheric branch of the hydrological cycle and climate. *Variations in the Global Water Budget*, Springer Netherlands, 5–65, https://doi.org/10.1007/978-94-009-6954-4_2, URL https://doi.org/10.1007/978-94-009-6954-4_2.

Qian, J.-H., 2008: Why precipitation is mostly concentrated over islands in the maritime continent. *Journal of the Atmospheric Sciences*, **65 (4)**, 1428–1441, https://doi.org/10.1175/2007JAS2422.1, URL https://journals.ametsoc.org/jas/article/65/4/1428/26793/Why-Precipitation-Is-Mostly-Concentrated-over.

Rodriguez-Iturbe, I., D. Entekhabi, and R. L. Bras, 1991: Nonlinear dynamics of soil moisture at climate scales: 1. stochastic analysis. *Water Resources Research*, **27**, 1899–1906, https://doi.org/10.1029/91WR01035.

Seneviratne, S. I., T. Corti, E. L. Davin, M. Hirschi, E. B. Jaeger, I. Lehner, B. Orlowsky, and A. J. Teuling, 2010: Investigating soil moisture–climate interactions in a changing climate: A review. **99 (3)**, 125–161, https://doi.org/10.1016/j.earscirev.2010.02.004, URL https://www.sciencedirect.com/science/article/pii/S0012825210000139.

Shannon, C. E., 1948: A mathematical theory of communication. *The Bell System Technical Journal*, **27 (3)**, 379–423, https://doi.org/10.1002/j.1538-7305.1948.tb01338.x.

Sobel, A. H., and G. Bellon, 2009: The effect of imposed drying on parameterized deep convection. *Journal of the Atmospheric Sciences*, **66 (7)**, 2085–2096, https://doi.org/10.1175/2008JAS2926.1, URL https://journals.ametsoc.org/view/journals/atsc/66/7/2008jas2926.1.xml.

Sobel, A. H., C. D. Burleyson, and S. E. Yuter, 2011: Rain on small tropical islands. *Journal of Geophysical Research: Atmospheres*, **116**, https://doi.org/10.1029/2010JD014695, URL https://agupubs.onlinelibrary.wiley.com/doi/abs/10.1029/2010JD014695.

Ulrich, M., and G. Bellon, 2019: Superenhancement of precipitation at the center of tropical islands. *Geophysical Research Letters*, **46 (24)**, 14 872–14 880, https://doi.org/10.1029/2019GL084947, URL https://agupubs.onlinelibrary.wiley.com/doi/abs/10.1029/2019GL084947.

Wang, S., and A. H. Sobel, 2017: Factors controlling rain on small tropical islands: Diurnal cycle, large-scale wind speed, and topography. *Journal of the Atmospheric Sciences*, **74 (11)**, 3515–3532, https://doi.org/10.1175/JAS-D-16-0344.1, URL https://journals.ametsoc.org/jas/article/74/11/3515/42168/Factors-Controlling-Rain-on-Small-Tropical-Islands.